

# A Millennial-Scale Oscillation in Latitudinal Temperature Gradients along the Western North Atlantic during the Mid-Holocene

Bryan N Shuman<sup>1</sup>, Ioana Cristina Stefanescu<sup>1</sup>, Laurie D Grigg<sup>2</sup>, David R Foster<sup>3</sup>, and W. Wyatt Oswald<sup>4</sup>

<sup>1</sup>University of Wyoming

<sup>2</sup>Norwich University

<sup>3</sup>Harvard Forest

<sup>4</sup>Emerson College

December 16, 2022

## Abstract

Changes in vegetation in North America indicate Holocene shifts in the latitudinal temperature gradient along the western margin of the North Atlantic. The dynamics of tree taxa such as oak (*Quercus*) and hickory (*Carya*) showed opposing directions of change across different latitudes, consistent with changes in temperature gradients. Pollen-inferred temperatures from 34 sites quantify the changes and reconstruct a long-term southward shift of the sharpest temperature gradient in winter and a northward shift in summer. During the mid-Holocene, however, an oscillation in tree distributions interrupted the trends indicating that the steepest portion of the seasonal temperature gradients migrated rapidly northward at 5.8-3.2 ka. The shift produced an unusually late summer thermal maxima at 42-43.5°N where oak abundance peaked both in the early and mid-Holocene. The changes appear consistent with orbital and ice sheet forcing as well as millennial variability in the North Atlantic pressure field during the mid-Holocene.

## Hosted file

952188\_0\_art\_1\_rmy51m.docx available at <https://authorea.com/users/566820/articles/613427-a-millennial-scale-oscillation-in-latitudinal-temperature-gradients-along-the-western-north-atlantic-during-the-mid-holocene>

## Hosted file

952188\_0\_supp\_10536825\_rmwbmn.docx available at <https://authorea.com/users/566820/articles/613427-a-millennial-scale-oscillation-in-latitudinal-temperature-gradients-along-the-western-north-atlantic-during-the-mid-holocene>

1  
2 **A Millennial-Scale Oscillation in Latitudinal Temperature Gradients along the**  
3 **Western North Atlantic during the Mid-Holocene**  
4

5 **Bryan N. Shuman<sup>1</sup>, Ioana C. Stefanescu<sup>1</sup>, Laurie D. Grigg<sup>2</sup>, David R. Foster<sup>3</sup>, and W.**  
6 **Wyatt Oswald<sup>4</sup>**

7 <sup>1</sup> Department of Geology and Geophysics, University of Wyoming, Laramie, WY.

8 <sup>2</sup> Department of Earth and Environmental Sciences, Norwich University, Northfield, VT.

9 <sup>3</sup> Harvard Forest, Harvard University, Petersham, MA.

10 <sup>4</sup> Marlboro Institute for Liberal Arts and Interdisciplinary Studies, Emerson College, Boston,  
11 MA.

12  
13 Corresponding author: Bryan Shuman (bshuman@uwyo.edu)  
14

15 **Key Points:**

- 16 • Winter and summer latitudinal temperature gradients changed during the Holocene in  
17 eastern North America, including at millennial scales.
- 18 • Temperature gradients responded to isolation, ice sheet extent, and millennial-scale  
19 dynamics similar to the North Atlantic Oscillation.
- 20 • Distributions of major tree taxa were sensitive to the changes, recording different  
21 direction changes at different latitudes.  
22  
23  
24  
25  
26  
27

**28 Abstract**

29 Changes in vegetation in North America indicate Holocene shifts in the latitudinal temperature  
30 gradient along the western margin of the North Atlantic. The dynamics of tree taxa such as oak  
31 (*Quercus*) and hickory (*Carya*) showed opposing directions of change across different latitudes,  
32 consistent with changes in temperature gradients. Pollen-inferred temperatures from 34 sites  
33 quantify the changes and reconstruct a long-term southward shift of the sharpest temperature  
34 gradient in winter and a northward shift in summer. During the mid-Holocene, however, an  
35 oscillation in tree distributions interrupted the trends indicating that the steepest portion of the  
36 seasonal temperature gradients migrated rapidly northward at 5.8-3.2 ka. The shift produced an  
37 unusually late summer thermal maxima at 42-43.5°N where oak abundance peaked both in the  
38 early and mid-Holocene. The changes appear consistent with orbital and ice sheet forcing as well  
39 as millennial variability in the North Atlantic pressure field during the mid-Holocene.

40

**41 Plain Language Summary**

42 In the Northern Hemisphere, average temperatures decline with latitude as climates cool toward  
43 to the pole. Changes in the temperature pattern have significant consequences for weather  
44 systems and the ecosystems affected by them. Summer warmth and winter freezing often  
45 determine where tree species can grow. As a result, fossils that show where trees grew in the past  
46 offer a unique perspective on past temperatures. In this study, changes in tree distributions over  
47 the past 11,700 years revealed that the northward decline in average temperatures near the  
48 Atlantic coast of North America fluctuated over time, illustrating a process involved in how  
49 climates varied from one millennium to the next. A particularly striking climate change at 5800-  
50 3200 years ago caused oak and hickory trees to increase in abundance in mid-latitudes, but  
51 decline to the north, steepening the difference between latitude bands. The forest histories  
52 demonstrate a strong sensitivity to climate variation, including rapid increases and decreases in  
53 tree populations that hint at patterns of a poorly understood timescale of climate variability.

54

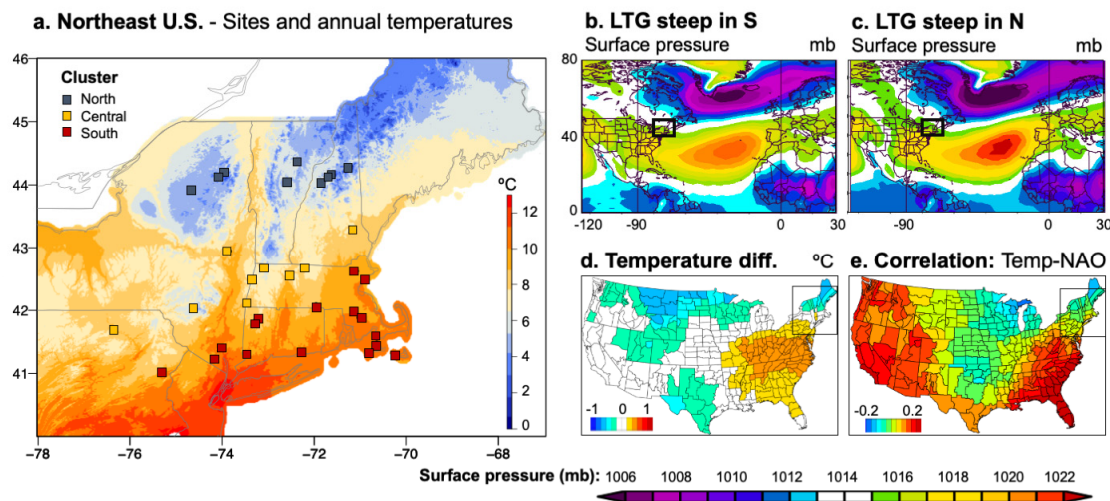
## 55 1 Introduction

56       Temperatures decline steeply with latitude in the northern mid-latitudes, particularly over  
57 the eastern areas of the continents. The areas of greatest change are associated with westerly jet  
58 streams and create eco-climatic transition zones, such as along the polar front (Bryson, 1966).  
59 The location of the front depends upon factors such as topography and land surface conditions  
60 (Pielke & Vidale, 1995; Seager et al., 2002), but climate variability such as the North Atlantic  
61 Oscillation (NAO) can modify the north-south temperature gradient and the location of its  
62 steepest transitions in both summer and winter (Folland et al., 2009; Hurrell et al., 2003). During  
63 the Holocene, external forcing also influenced latitudinal temperature gradients with  
64 consequences for terrestrial ecosystems (Davis & Brewer, 2009; Routson et al., 2019). Potential  
65 variations at centennial to millennial scales have been hard to diagnose (Crucifix et al., 2017;  
66 Hernández et al., 2020), but may have been particularly important in the North Atlantic region  
67 (O'Brien et al., 1995; Olsen et al., 2012; Orme et al., 2021; Shuman et al., 2019). Reconstructing  
68 variations in the latitudinal temperature gradient (LTG), however, could help to evaluate the  
69 dynamics driving centennial to millennial climate variations and their ecological consequences.

70       Holocene tree species' distributions indicate past LTG changes because both growing  
71 season warmth and winter freezing temperatures strongly influence plant ranges (Prentice et al.,  
72 1991; Woodward, 1987). Centennial-to-millennial temperature changes likely drove shifts in  
73 species abundance within previously established tree distributions (Fletcher et al., 2013; Foster et  
74 al., 2006; Marsicek et al., 2013). In the North Atlantic region, biogeographic changes can arise  
75 from regional LTG responses to the atmospheric pressure difference between the Icelandic low  
76 and the North Atlantic sub-tropical high (Hurrell & Deser, 2010). Both pressure systems vary in  
77 strength on seasonal (Portis et al., 2001) to orbital time scales (Alder & Hostetler, 2015), likely  
78 including centennial to millennial scales (Olsen et al., 2012; Orme et al., 2021). Today, a weak  
79 N-S pressure gradient (negative NAO) shifts the steepest portion of the LTG in eastern North  
80 America southward as boreal regions warm (Figure 1b), whereas a strong gradient (positive  
81 NAO) does the reverse because mid-latitude North America warms (Figure 1c). NAO-like  
82 variations at millennial scales could link climate and ecosystem changes in the North Atlantic  
83 (Giraudeau et al., 2010; Larsen et al., 2012; Orme et al., 2021), Europe (Fletcher et al., 2013;  
84 Vanni re et al., 2011), and North America (Shuman, 2022).

85       To help constrain the synoptic patterns of such climate variations, we used fossil pollen  
86 to reconstruct Holocene changes in the LTG over eastern North America. In this region, changes  
87 in the LTG during the Pleistocene and early-Holocene depended on the state of the North  
88 Atlantic (Fastovich et al., 2020; Levesque et al., 1997; Ruddiman & McIntyre, 1981) and later on  
89 the demise of the Laurentide ice sheet and its glacial anti-cyclone (COHMAP, 1988; Shuman et  
90 al., 2002). Additional less well diagnosed changes continued into the mid- and late-Holocene.  
91 Kirby et al. (2002) used lake oxygen isotopes to infer a rapid southward shift in the polar front in  
92 the mid-Holocene. Pollen records show abrupt changes at the same time (Willard et al., 2005).  
93 Pollen-inferred summer temperatures declined abruptly at ca. 5 ka across the northern U.S. when  
94 they increased 1) to the south from the Great Plains to southern New England (Shuman, 2022;  
95 Shuman & Marsicek, 2016) and 2) on average across Europe and North America (Marsicek et  
96 al., 2018). Sea-surface temperature reconstructions document different directions of temperature  
97 change across latitudes in the western Atlantic at the same time (Lochte et al., 2020; Schmidt et  
98 al., 2012).

99



100

101 **Figure 1. Maps of a) the location of fossil pollen sites, b) years with a steep latitudinal**  
 102 **pressure gradient (LTG) in the northern part of the study region (inset box), c) years with**  
 103 **a steep LTG in the southern part, d) the mean annual temperature difference between the**  
 104 **two sets of years, and e) the annual temperature correlation with the NAO. Modern mean**  
 105 **annual temperature across the region (a) are based on 1991-2020 PRISM normals (PRISM**  
 106 **2020); symbols indicate the geographical cluster containing each fossil site. Maps of**  
 107 **composite mean surface atmospheric pressures show years when the LTG was steepest b)**  
 108 **south of 42.75°N (1960, 1977, 1988, 1999, 2001) and c) north of 42.75°N (1954, 1959, 1968,**  
 109 **1991, 2007). Lower maps represent the d) composite mean temperature differences**  
 110 **between each set of years and e) the correlation coefficient,  $r$ , between the NAO and mean**  
 111 **annual temperature ( $T$ ) in each U.S. climate division (Vose et al., 2014).**

112 Here, we reconstruct the Holocene position of the steepest portion of LTG across the  
 113 northeast U.S. where it is sensitive to the NAO and where modern mean annual temperatures  
 114 range from  $<2^{\circ}\text{C}$  to  $>12^{\circ}\text{C}$  (Fig. 1). Fossil pollen records in the study region closely track the  
 115 climate history (Shuman et al., 2019) and document changes in a strong N-S vegetation gradient  
 116 (Oswald et al., 2018), which expressed a close association with temperature at the time of  
 117 European colonization (Cogbill et al., 2002; Thompson et al., 2013). We, therefore, use a dense  
 118 network of 34 pollen stratigraphies to infer summer and winter temperature history at different  
 119 latitudes across the region. Latitudinal contrasts in the history of two representative tree genera,  
 120 oak (*Quercus*) and hickory (*Carya*), underpin the inferred changes in the LTG and highlight the  
 121 ecological significance of potential millennial-scale climate variability near the North Atlantic.

## 122 2 Methods

123 Detailed fossil pollen records from Connecticut, Massachusetts, New Hampshire, New  
 124 York, Pennsylvania, and Vermont were obtained from the Neotoma Paleocological Database  
 125 (Williams et al., 2018). The records were selected from areas that span the full north-south  
 126 temperature contrast between 40-45°N latitude. This range of latitudes was possible from 70-

127 77°W longitude, but not in places to the east, such as Maine. The records span the full Holocene  
128 and contain an average of 72 fossil pollen samples (Table S1). Chronologies were updated using  
129 *intcal20* in *bchron* (Parnell et al., 2008; Reimer et al., 2020).

130 We reconstructed mean summer (June-August) and winter (December-February)  
131 temperatures using the modern analog technique following the methods of Marsicek et al.  
132 (2013), which compared each fossil sample to the best modern analogs from North America east  
133 of 95°W using the squared-chord distance metric (Overpeck et al., 1985). The modern pollen  
134 samples and their associated temperatures derive from Whitmore et al. (2005). For each fossil  
135 pollen sample, the temperatures of the best seven modern analogs were averaged to produce the  
136 reconstructed temperature using the R package, *rioja* (Juggins, 2019).

137 Hierarchical cluster analysis of the summer temperature reconstructions (*hclust* based on  
138 Euclidean distances in R)(R Core Development Team, 2022) was used to group the individual  
139 records into three ensembles. The clusters were determined from the consistency in their summer  
140 temperature reconstructions, which break out by latitude with northern (>43.5°N), central (42-  
141 43.5°N), and southern (<42°N) groups of sites, except that eastern coastal sites tended to cluster  
142 with the southern group (Fig. 1a). The LTG reconstructions were based on the averages of  
143 individual records within each ensemble to reduce reconstruction and chronological uncertainties  
144 and remove local ecological effects and noise. Reconstructions were first interpolated to 50-yr  
145 intervals to enable averaging on a consistent time scale.

146 The north-south gradient was measured by assuming that cluster means represent the  
147 average temperatures of the three latitudinal bands. The strength of the LTG was calculated as  
148 the change in temperature between bands by measuring the central-northern (C-N) and southern-  
149 central (S-C) temperature differences; in each case, we subtracted the northern (cooler) cluster  
150 mean from the southern (warmer) cluster mean. The two segments were then compared to detect  
151 where the LTG was steepest by subtracting the C-N and S-C differences from each other.  
152 Positive values in the C-N minus S-C difference indicate a steeper gradient north of 42.75°N, the  
153 mid-point of the region, and negative values indicate a steeper gradient to the south.

154 As context, modern changes in the LTG (shown in Fig. 1) were calculated using the same  
155 approach by using annual temperatures from climate division data (Vose et al., 2014);  
156 temperature data from Vermont (statewide mean), western Massachusetts (division 1), and  
157 Connecticut (statewide mean) represent the northern, central, and southern cluster regions  
158 respectively. Composite anomaly maps showing changes in surface pressure and temperatures  
159 were generated using the NCEP/NCAR Reanalysis (Kalnay et al., 1996) for the five years when  
160 the steepest gradient was furthest north or south based on the C-N (MA-VT) minus S-C (CT-  
161 MA) difference, and mapped using tools from the NOAA/ESRL Physical Sciences Laboratory,  
162 Boulder, Colorado at <https://psl.noaa.gov/>.

### 163 **3 Results**

#### 164 **3.1 Reconstructed temperature trends**

165 All of the temperature reconstructions indicate significant early Holocene warming in  
166 both summer (Fig. 2) and winter (Fig. 3). At the end of the Younger Dryas at ca. 11.7 ka,  
167 summer temperatures increased from 15-16°C to 17.5-18.5°C with all latitudes warming by  
168 similar amounts. Summer warming peaked at 18-19°C in the central and northern sites by 8 ka,  
169 but southern sites continued to warm, reaching 21°C at 5.5 ka (Fig. 2). In winter, all three

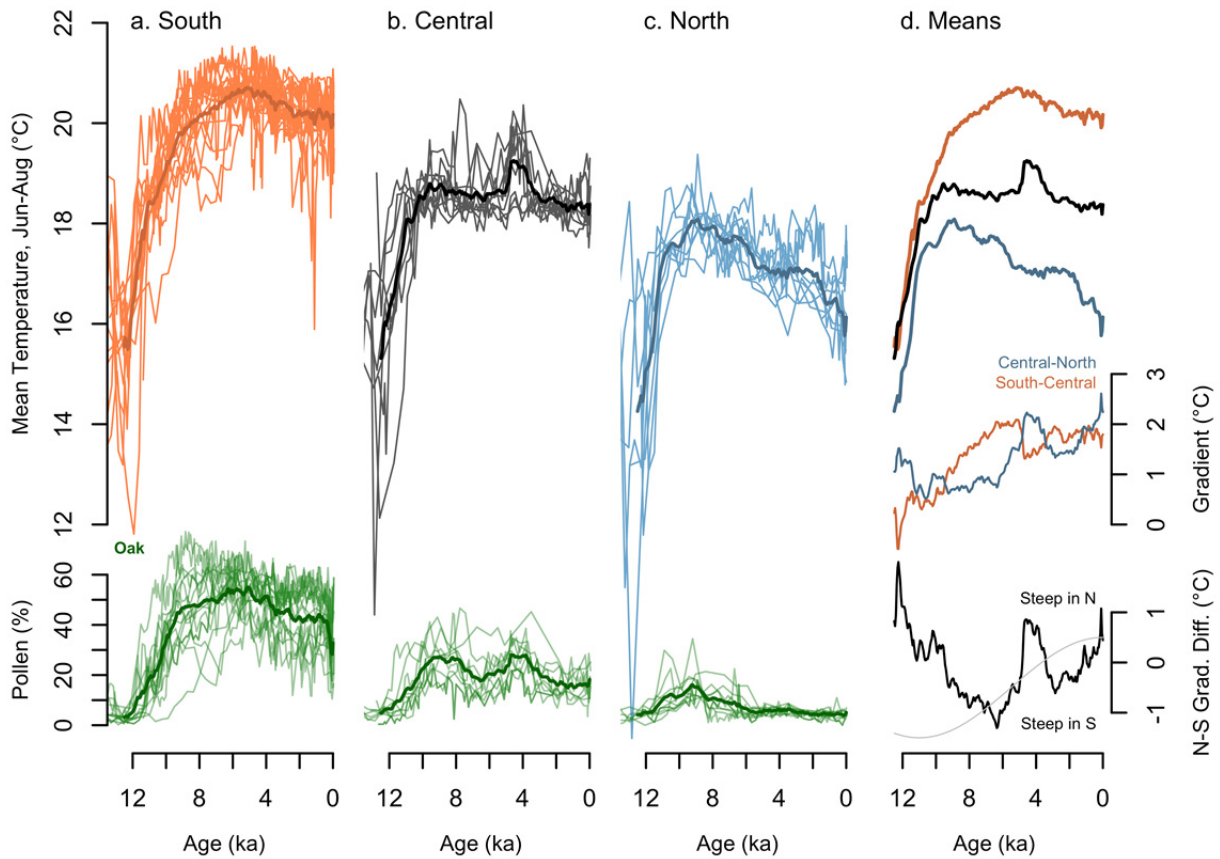
170 regions continued to warm until 5.5 ka with the greatest rate of warming immediately following  
171 the Younger Dryas when all areas increased from  $<-10^{\circ}\text{C}$  to  $>-7^{\circ}\text{C}$  (Fig. 3). After 10 ka, the  
172 southern sites warmed faster in winter than the central and northern sites; by 5.5 ka, southern  
173 sites reached near freezing ( $0^{\circ}\text{C}$ ) even though northern areas only warmed to  $-5^{\circ}\text{C}$  (Fig. 3).

174 After the mid-Holocene, summer temperatures declined in both the northern and southern  
175 regions, but not at central sites, which were affected by a significant millennial-scale variation  
176 after 5.8 ka (Fig. 2). Initially, northern sites cooled by  $0.5^{\circ}\text{C}$  in both summer (Fig. 2) and winter  
177 (Fig. 3). Then, from 4.5-3.2 ka, central sites warmed by  $0.5^{\circ}\text{C}$  in summer (Fig. 2) and  $1^{\circ}\text{C}$  in  
178 winter (Fig. 3). After 3.2 ka, northern temperatures remained low in summer, but they warmed  
179 again in winter. A second rapid cooling of  $0.5^{\circ}\text{C}$  at 1.5 ka further prevented many northern sites  
180 from returning to their previous high summer temperatures.

### 181 3.2 Reconstructed gradient changes

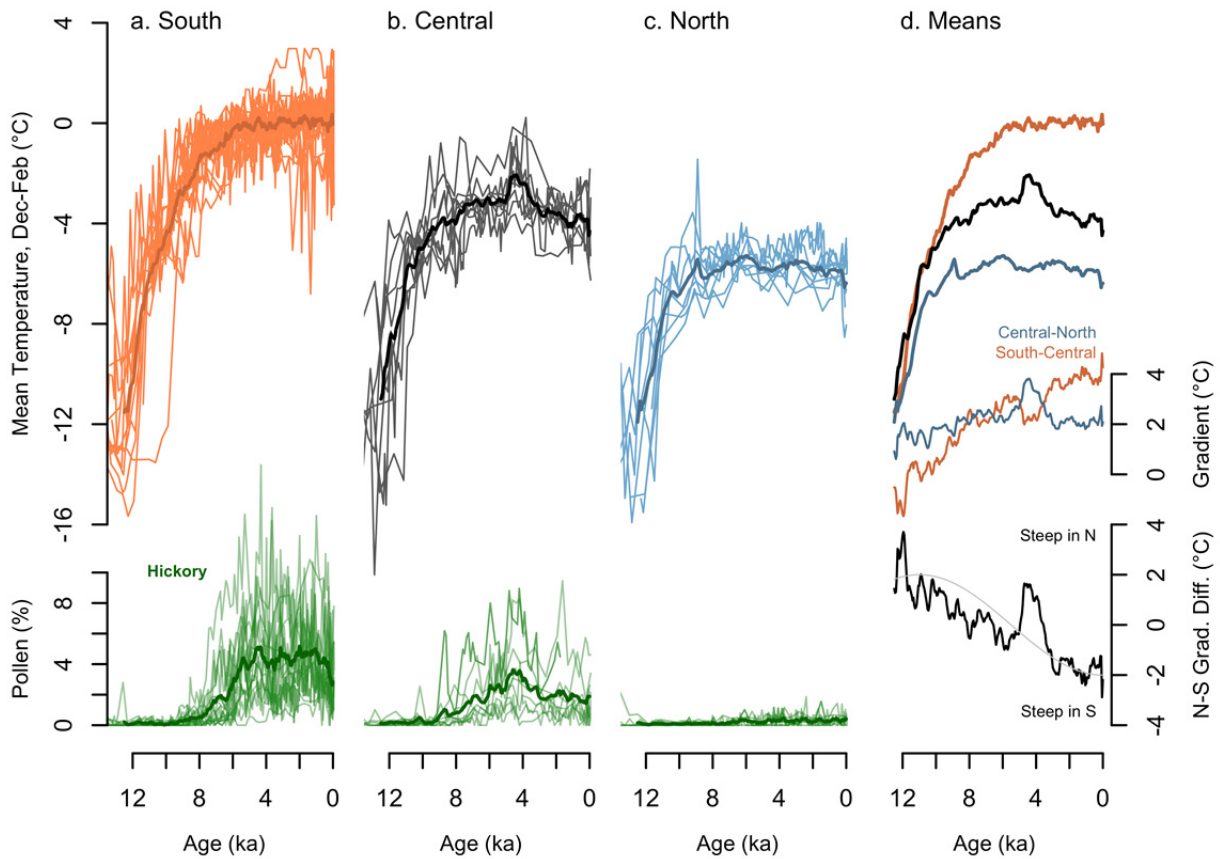
182 The differences between latitudinal clusters indicate that the regional LTG increased over  
183 much of the Holocene (Fig. 2d, 3d). Qualitative interpretation of the fossil pollen record also  
184 indicates such gradient changes. Oak (*Quercus*), a warmth-adapted genus of broadleaved  
185 deciduous trees that flourishes today where summer temperatures exceed  $17^{\circ}\text{C}$  (Williams et al.,  
186 2006), increased until ca. 5.5 ka at the southern cluster of sites, but had reached its maximum in  
187 the north by 9-8 ka (Fig. 2, green lines). Northern abundance fell to near zero before the 5.5 ka  
188 peak was achieved in the south. The opposite patterns of change in oak abundance from 9-5.5 ka,  
189 observed over many sites, indicate a widening difference in growing conditions between north  
190 and south. The temperature reconstructions based on the full pollen assemblages indicate that the  
191 temperature difference increased by  $1-1.5^{\circ}\text{C}$  (Fig. 2d).

192 A second millennial-scale peak in oak abundance in the central region from 4.6-3.2 ka  
193 developed when oak abundance began declining in the south and remained low in the north (Fig.  
194 2, green lines). Consequently, the history of oak indicates a weakening of the southern vegetation  
195 and summer temperature gradients from 4.6-3.2 ka as they became steep in the north. The  
196 reconstructions indicate that the mid-Holocene anomaly sharply reduced the apparent summer  
197 gradient in the south (S-C) by  $0.5^{\circ}\text{C}$  as the northern gradient (C-N) increased by  $>1^{\circ}\text{C}$  (Fig. 2d).



198

199 **Figure 2. Mean summer (June-August) temperatures and oak (*Quercus*) pollen percentages**  
 200 **from a) southern, b) central, and c) northern sites. d) Mean reconstructions for each cluster**  
 201 **(bold lines) are shown with their differences and the north minus south difference in**  
 202 **gradient steepness (“N-S Grad. Diff.” as the black line at bottom right). Positive gradient**  
 203 **differences indicate a steeper gradient in the north and negative values indicate steeper in**  
 204 **the south. An inverted Northern Hemisphere June insolation curve (Berger, 1978) is**  
 205 **normalized to the gradient difference scale for comparison (thin line).**



206

207 **Figure 3. As in Figure 2, but for mean winter (December-February) temperatures and**  
 208 **hickory (*Carya*) pollen). A Northern Hemisphere January insolation (inverted, gray line)**  
 209 **is normalized to the N-S gradient difference in d for comparison.**

210 The reconstructed gradients also changed in winter. The patterns appear qualitatively in  
 211 the Holocene history of hickory (*Carya*), a genus of broadleaved deciduous trees usually  
 212 restricted in the study area today to areas with mean winter temperatures greater than  $-4^{\circ}\text{C}$   
 213 (Williams et al., 2006). Unlike oak, hickory is a statistically minor taxon and only became  
 214 important in the study area after ca. 8 ka (green lines, Fig. 3). Its history parallels the slower  
 215 long-term increase in temperatures during winter compared to summer. As oak and summer  
 216 temperatures declined in the late Holocene, hickory retained its earlier abundance suggesting  
 217 stable winter temperatures.

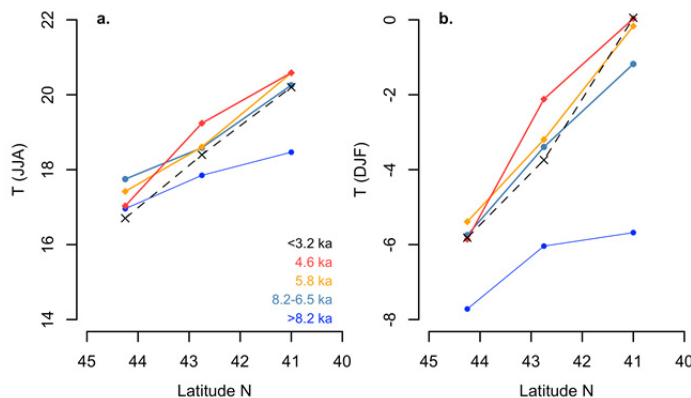
218 The increase in hickory in the south after 8 ka, but not in the north, marks a widening  
 219 latitudinal vegetative difference and is reflected by the winter temperature reconstructions  
 220 generated from the full pollen assemblages. The reconstructions show a persistent C-N  
 221 difference of  $\sim 2^{\circ}\text{C}$  (thin blue line, Fig. 3d), but a widening S-C difference from near-zero to  
 222  $>4^{\circ}\text{C}$  (thin red line, Fig. 3d). An exception to this pattern developed from 4.6-3.2 ka when  
 223 hickory abundance increased in the central region as oak-hickory assemblages typical of the  
 224 south expanded into central highland sites. Corresponding winter temperature reconstructions  
 225 indicate a  $2^{\circ}\text{C}$  increase in the C-N gradient and a  $\sim 1^{\circ}\text{C}$  decline in the S-C gradient (Fig. 3d).

## 226 3.3 Changing latitude of steepest gradients

227 The difference in the steepness of the two summer temperature gradients (the C-N minus  
 228 S-C gradient difference, bottom panel, Fig. 2d) indicates

- 229 • a southward shift in the steepest part of the gradient before 6 ka as the C-N difference  
 230 remained stable but the S-C difference increased;
- 231 • a millennial oscillation from 4.6-3.2 ka when the northern (C-N) gradient became steeper  
 232 than the southern (S-C) gradient by up to 0.8°C; and then
- 233 • a northward shift in the steepest portion of the gradient (a positive gradient difference,  
 234 Fig. 2d) after 3.2 ka.

235 In winter, because the northern (C-N) gradient remained near 2°C and the southern (S-C)  
 236 gradient increased from 0°C to >4°C, the gradient was initially steepest in the north but shifted to  
 237 the south, even following the northward oscillation from 4.6-3.2 ka when C-N was steeper than  
 238 S-C by up to 1.6°C (Fig. 3d).



239

240 **Figure 4. Reconstructed latitudinal temperatures for a) summer (July-August, JJA) and b)**  
 241 **winter (December-February, DJF) on average at >8.2 ka (dark blue), from 8.2-6.5 ka (light**  
 242 **blue), and since 3.2 ka (black) for comparison with those at 5.8 ka (orange) and 4.6 ka**  
 243 **(red).**

244 **4 Discussion**

## 245 4.1 Interpreting the vegetation changes

246 A modern association between ecotones and the steepest fronts in the LTG has long been  
 247 recognized (Bryson, 1966; Pielke & Vidale, 1995). At the time of European colonization of the  
 248 northeastern U.S., the LTG determined a sharp contrast between northern mixed forests and oak-  
 249 hickory forests to the south (Cogbill et al., 2002). Oak and hickory had similar distributions in  
 250 the study region at the time, but their different seasonal temperature sensitivities are underscored  
 251 by strikingly different historic distributions in the central U.S. where continental summer and  
 252 winter temperature patterns differ, limiting hickory's northern extent (Paciorek et al., 2016,  
 253 2021; Prentice et al., 1991). The Holocene abundances of these and other regional tree taxa have  
 254 similarly been linked to temperature changes since the earliest palynological studies (Deevey,  
 255 1939). Indeed, direct comparisons between fossil pollen and independent paleoclimate data from

256 the northeast U.S. reveal a tight coupling with no significant lags at >100 yr time scales (Shuman  
257 et al., 2019).

258 The reconstructed shifts in the LTG, therefore, provide a plausible climatic explanation  
259 for spatial differences in the histories of warm-tolerant oak and hickory populations among  
260 others. A weak north-south gradient in summer before ca. 6.5 ka (light blue line, Figure 4a) helps  
261 to explain the early peak in oak abundance at northern sites (green lines, Figure 2c); the polar  
262 front was likely furthest north at the time, extending similar summer temperatures across the  
263 region and enabling oak to spread widely. If the summer LTG then steepened by 5.8 ka (Figure  
264 2d), oak could have readily declined where sites began cooling in the north (Figure 2c) while  
265 expanding into newly warmed central areas (Figure 2b). Tree population increases south of a  
266 non-advancing range limit are not uncommon (Lloyd, 2005), especially if the LTG were to  
267 steepen rather than to produce uniform temperatures increases or declines regionwide (Figure 4).

268 Other alternative interpretations do not explain the spatial complexity of the observed  
269 vegetation changes. For example, dispersal lags would not have been important because oak and  
270 hickory were established across the study area early in the Holocene. Ecological and statistical  
271 percentage effects of a range-wide decline of hemlock (*Tsuga*) populations at ca. 5.5-5.0 ka also  
272 should have applied across the entire region and do not explain why oak would have increased  
273 only in the central region while declining in others (Foster et al., 2006). Climatic influences  
274 rather than short-lived successional dynamics also clarify why oak increased at 4.6-3.2 ka after  
275 shade-tolerant, late-successional taxa like beech (*Fagus*) increased at the same sites from 5.0-4.6  
276 ka (Oswald et al., 2007, 2018; Whitehead & Crisman, 1978). Additionally, the modern analog  
277 technique used here simultaneously produces independently-validated precipitation  
278 reconstructions (Shuman et al., 2019) and accounts for the interacting role of moisture on the  
279 pollen assemblages when reconstructing temperatures (Williams and Shuman 2008).

#### 280 4.2 Climate dynamics involved

281 Different directions of insolation forcing over the Holocene explain much of the  
282 northward steepening of the summer LTG (Fig. 2d) and southward steepening of the winter LTG  
283 (Fig. 3d). Early-to-mid Holocene insolation anomalies acted to weaken the summer LTG (Fig.  
284 4a) by preferentially heating northern continental areas, especially compared to coastal areas in  
285 the south. The winter LTG also strengthened since the early Holocene (Fig. 4b) because  
286 insolation anomalies cooled low latitudes more than high latitudes, which receive little winter  
287 insolation even today (Berger, 1978). A southward shift in the summer LTG during the early-  
288 Holocene, however, represents a departure from the insolation trend (black line, bottom, Fig. 2d).  
289 Much of the change, prior to ca. 8 ka, appears consistent with a weak north-south pressure  
290 gradient when the Laurentide ice sheet remained influential. The summer anomaly may conflict  
291 with expectations of an insolation-driven strengthening of the pressure gradient (Alder &  
292 Hostetler, 2015), but could indicate that a thermodynamic response to the ice albedo anomaly  
293 likely generated the pattern (Morrill et al., 2018) rather than the year-round effect of the ice as a  
294 mechanical barrier to the flow of the jet stream (COHMAP, 1988).

295 The most significant departure from the insolation and ice sheet effects arises as a  
296 pronounced northward shift in the steepest portion of the gradient after 5.8 ka. Despite the  
297 opposing directions of long-term change between seasons in the late-Holocene, the summer and  
298 winter expression of the mid-Holocene oscillation were similar. The similar patterns may relate  
299 to challenges separately reconstructing climate variables that are correlated today, but the large

300 differences in the summer and winter LTG reconstructions overall indicate that the anomaly may  
301 well apply to both seasons. Both anomalies began as temperatures fell in the north at 5.8 ka (bold  
302 blue lines, Fig. 2d, 3d) and were then amplified when temperatures in the central region  
303 increased sharply at 4.8-3.7 ka (bold black lines, Fig. 2d, 3d). The initial cooling at northern sites  
304 agrees with isotopic evidence from northern sites (Kirby et al., 2002; Shuman & Marsicek,  
305 2016). Such a steepening and northward shift in the LTG develops during positive summer NAO  
306 phases today (Folland et al., 2009). Temperature anomalies today develop in central areas, such  
307 as western Massachusetts, as an extension of warming in the mid-Atlantic region, but are  
308 surrounded by little change in the southern part of our study area (Fig. 1d).

309 Low sea-surface temperatures (SSTs) from 4.5-3.5 ka on the Labrador Shelf (Lochte et  
310 al., 2020) and coincident high SSTs in the Florida Strait from 4.7-3.3 ka (Schmidt et al., 2012)  
311 agree with the anti-phased SST anomalies along the North American margin expected from  
312 patterns associated with a strong Atlantic pressure gradient (Fig. S1). However, a correlated  
313 NAO reconstruction from lake sediments in Greenland records the opposite sign phase (Olsen et  
314 al., 2012), which raises questions about the specific circulation changes involved and whether  
315 they have direct analogs to the NAO at monthly to annual scales. Regardless of the relationship  
316 to NAO phases or not, the oscillation coincides with prominent features in other North Atlantic  
317 records, which indicate millennial anomalies in deep water flow, wind speeds, and atmospheric  
318 circulation (Giraudeau et al., 2010; Jackson et al., 2005; O'Brien et al., 1995) when evidence of  
319 unusual climates extended from submerged tree stumps in Lake Tahoe, California (Benson et al.,  
320 2002) and paleosol development in Nebraska's Sand Hills (Miao et al., 2007) to millennial  
321 temperature and isotopic anomalies in Africa (Berke et al., 2012; Thompson et al., 2002).

322 The millennial-scale shifts in the LTG and Atlantic pressure gradient may relate to  
323 intrinsic atmospheric variability on interannual time scales (Folland et al., 2009; Hurrell et al.,  
324 2003), particularly given the potential involvement of ocean-atmosphere or sea-ice interactions  
325 to sustain variations over centuries to millennia during the mid-Holocene (Orme et al., 2021;  
326 Rigor et al., 2002; Thornalley et al., 2009). Alternatively, volcanic and solar variability may have  
327 been influential factors (Fletcher et al., 2013; Kobashi et al., 2017), but no clear linear correlation  
328 with external forcing is evident, potentially as expected (Renssen et al., 2006).

## 329 **5 Conclusions**

330 The Holocene temperature history of eastern North America includes changes in the  
331 steepness of the north-south temperature gradient, which generally responded in different  
332 directions to summer and winter insolation anomalies. Well-described Holocene forcing,  
333 however, does not explain an apparent millennial-scale latitudinal shift in the slope and position  
334 of the temperature front, which expanded oak-hickory forests into mid-latitudes as they declined  
335 to the north from 5.8-3.2 ka. Understanding the NAO-like change may help explain other mid-  
336 Holocene abrupt change events and dynamics.

337

338 **Acknowledgments**

339 This work was supported by NSF funding to BNS (DEB-1856047) and to the Harvard Forest  
340 Long-Term Ecological Research Program (LTER-1832210).

341

342 **Open Research**

343 The analyses here depend upon fossil pollen data, which can be retrieved from the Neotoma  
344 Paleocology Database using the site names listed in Table S1 in the 'neotoma' package version  
345 1.7.4 in R 4.0.0 (Goring et al., 2019; R Core Development Team, 2022). Chronologies were updated  
346 in R using the 'bchron' package version 4.7.4 (Parnell et al., 2008) and temperature reconstructions  
347 were generated using the 'rioja' package version 0.9-21 (Juggins, 2019). The reconstructions and  
348 median ages are available as a supplement to this manuscript and will be submitted to the NOAA  
349 NCEI Paleoclimate archive upon acceptance for publication.

350

351 **References**

- 352 Alder, J. R., & Hostetler, S. W. (2015). Global climate simulations at 3000-year intervals for the last 21 000 years  
353 with the GENMOM coupled atmosphere–ocean model. *Climate of the Past*, *11*(3), 449–471.
- 354 Benson, L., Kashgarian, M., Rye, R., Lund, S., Paillet, F., Smoot, J., et al. (2002). Holocene multidecadal and  
355 multicentennial droughts affecting Northern California and Nevada. *Quaternary Science Reviews*, *21*(4–6),  
356 659–682.
- 357 Berger, A. (1978). Long-term variations of caloric insolation resulting from the earth's orbital elements. *Quaternary*  
358 *Research*, *9*(2), 139–167.
- 359 Berke, M. A., Johnson, T. C., Werne, J. P., Schouten, S., & Sinninghe Damsté, J. S. (2012). A mid-Holocene  
360 thermal maximum at the end of the African Humid Period. *Earth and Planetary Science Letters*, *351–352*,  
361 95–104. <https://doi.org/10.1016/j.epsl.2012.07.008>
- 362 Bryson, R. A. (1966). Air masses, streamlines, and the boreal forest. *Geological Society of America Bulletin*, *8*, 228.

- 363 Cogbill, C. V., Burk, J., & Motzkin, G. (2002). The forests of presettlement New England, USA: spatial and  
 364 compositional patterns based on town proprietor surveys. *Journal of Biogeography*, 29(10–11), 1279–1304.  
 365 <https://doi.org/10.1046/j.1365-2699.2002.00757.x>
- 366 COHMAP Members (1988). Climate changes of the last 18,000 years: observations and model simulations. *Science*,  
 367 241, 1043–1052.
- 368 Crucifix, M., de Vernal, A., Franzke, C., & von Gunten, L. (2017). Centennial to Millennial Climate Variability,  
 369 131–166. <https://doi.org/10.22498/pages.25.3>
- 370 Davis, B. A., & Brewer, S. (2009). Orbital forcing and role of the latitudinal insolation/temperature gradient.  
 371 *Climate Dynamics*, 32(2–3), 143–165. <http://dx.doi.org/10.1007/s00382-008-0480-9>
- 372 Deevey, E. S. (1939). Studies on Connecticut lake sediments. I. A Postglacial Climatic Chronology for Southern  
 373 New England. *American Journal of Science*, 237, 691–724.
- 374 Fastovich, D., Russell, J. M., Jackson, S. T., Krause, T. R., Marcott, S. A., & Williams, J. W. (2020). Spatial  
 375 Fingerprint of Younger Dryas Cooling and Warming in Eastern North America. *Geophysical Research*  
 376 *Letters*, 47(22), e2020GL090031. <https://doi.org/10.1029/2020GL090031>
- 377 Fletcher, W. J., Debret, M., & Goñi, M. F. S. (2013). Mid-Holocene emergence of a low-frequency millennial  
 378 oscillation in western Mediterranean climate: Implications for past dynamics of the North Atlantic  
 379 atmospheric westerlies. *The Holocene*, 23(2), 153–166. <https://doi.org/10.1177/0959683612460783>
- 380 Folland, C. K., Knight, J., Linderholm, H. W., Fereday, D., Ineson, S., & Hurrell, J. W. (2009). The Summer North  
 381 Atlantic Oscillation: Past, Present, and Future. *Journal of Climate*, 22(5), 1082–1103.  
 382 <https://doi.org/10.1175/2008JCLI2459.1>
- 383 Foster, D. R., Oswald, W. W., Faison, E. K., Doughty, E. D., & Hansen, B. C. S. (2006). A climatic driver for abrupt  
 384 mid-Holocene vegetation dynamics and the hemlock decline in New England. *Ecology*, 87(12), 2959–2966.
- 385 Giraudeau, J., Grelaud, M., Solignac, S., Andrews, J. T., Moros, M., & Jansen, E. (2010). Millennial-scale  
 386 variability in Atlantic water advection to the Nordic Seas derived from Holocene coccolith concentration  
 387 records. *Quaternary Science Reviews*, 29(9), 1276–1287. <https://doi.org/10.1016/j.quascirev.2010.02.014>
- 388 Goring, S. J., Simpson, G. L., Marsicek, J. P., Ram, K., & Sosalla, L. (2019). neotoma: Programmatic R interface to  
 389 the Neotoma Paleoecological Database. R, rOpenSci. Retrieved from <https://github.com/ropensci/neotoma>

- 390 Hernández, A., Martín-Puertas, C., Moffa-Sánchez, P., Moreno-Chamarro, E., Ortega, P., Blockley, S., et al. (2020).  
 391 Modes of climate variability: Synthesis and review of proxy-based reconstructions through the Holocene.  
 392 *Earth-Science Reviews*, 209, 103286. <https://doi.org/10.1016/j.earscirev.2020.103286>
- 393 Hurrell, J. W., & Deser, C. (2010). North Atlantic climate variability: The role of the North Atlantic Oscillation.  
 394 *Journal of Marine Systems*, 79(3), 231–244. <https://doi.org/10.1016/j.jmarsys.2009.11.002>
- 395 Hurrell, J. W., Kushnir, Y., Ottersen, G., & Visbeck, M. (2003). *The North Atlantic Oscillation. Geophys. Monogr. Ser.* (Vol. 134). <https://doi.org/10.1029/134GM01>
- 397 Jackson, M. G., Oskarsson, N., Trønnnes, R. G., McManus, J. F., Oppo, D. W., Grönvold, K., et al. (2005). Holocene  
 398 loess deposition in Iceland: Evidence for millennial-scale atmosphere-ocean coupling in the North Atlantic.  
 399 *Geology*, 33(6), 509–512. <https://doi.org/10.1130/G21489.1>
- 400 Juggins, S. (2019). rioja: Analysis of Quaternary Science Data (Version 0.9-21). Retrieved from [https://CRAN.R-](https://CRAN.R-project.org/package=rioja)  
 401 [project.org/package=rioja](https://CRAN.R-project.org/package=rioja)
- 402 Kalnay, E., Kanamitsu, M., Kistler, R., Collins, W., Deaven, D., Gandin, L., et al. (1996). The NCEP/NCAR 40-  
 403 Year Reanalysis Project. *Bulletin of the American Meteorological Society*, 77(3), 437–472.  
 404 [https://doi.org/10.1175/1520-0477\(1996\)077<0437:TNYRP>2.0.CO;2](https://doi.org/10.1175/1520-0477(1996)077<0437:TNYRP>2.0.CO;2)
- 405 Kirby, M. E., Mullins, H. T., Patterson, W. P., & Burnett, A. W. (2002). Late glacial-Holocene atmospheric  
 406 circulation and precipitation in the northeast United States inferred from modern calibrated stable oxygen  
 407 and carbon isotopes. *Geological Society of America Bulletin*, 114(10), 1326–1340.  
 408 [https://doi.org/10.1130/0016-7606\(2002\)114<1326:lghaca>2.0.co;2](https://doi.org/10.1130/0016-7606(2002)114<1326:lghaca>2.0.co;2)
- 409 Kobashi, T., Menviel, L., Jeltsch-Thömmes, A., Vinther, B. M., Box, J. E., Muscheler, R., et al. (2017). Volcanic  
 410 influence on centennial to millennial Holocene Greenland temperature change. *Scientific Reports*, 7(1),  
 411 1441. <https://doi.org/10.1038/s41598-017-01451-7>
- 412 Larsen, D. J., Miller, G. H., Geirsdóttir, Á., & Ólafsdóttir, S. (2012). Non-linear Holocene climate evolution in the  
 413 North Atlantic: a high-resolution, multi-proxy record of glacier activity and environmental change from  
 414 Hvítárvatn, central Iceland. *Quaternary Science Reviews*, 39, 14–25.  
 415 <https://doi.org/10.1016/j.quascirev.2012.02.006>
- 416 Levesque, A. J., Cwynar, L. C., & Walker, I. R. (1997). Exceptionally steep north-south gradients in lake  
 417 temperatures during the last deglaciation. *Nature*, 385(6615), 423–426.

- 418 Lloyd, A. H. (2005). Ecological histories from Alaskan tree lines provide insight into future change. *Ecology*, *86*(7),  
 419 1687–1695.
- 420 Lochte, A. A., Schneider, R., Kienast, M., Repschläger, J., Blanz, T., Garbe-Schönberg, D., & Andersen, N. (2020).  
 421 Surface and subsurface Labrador Shelf water mass conditions during the last 6000 years. *Climate of the*  
 422 *Past*, *16*(4), 1127–1143. <https://doi.org/10.5194/cp-16-1127-2020>
- 423 Marsicek, J. P., Shuman, B., Brewer, S., Foster, D. R., & Oswald, W. W. (2013). Moisture and temperature changes  
 424 associated with the mid-Holocene *Tsuga* decline in the northeastern United States. *Quaternary Science*  
 425 *Reviews*, *80*(3), 333–342. <https://doi.org/10.1016/j.quascirev.2013.09.001>
- 426 Marsicek, J. P., Shuman, B. N., Bartlein, P. J., Shafer, S. L., & Brewer, S. (2018). Reconciling divergent trends and  
 427 millennial variations in Holocene temperatures. *Nature*, *554*(7690), 92–96.  
 428 <https://doi.org/10.1038/nature25464>
- 429 Miao, X., Mason, J. A., Johnson, W. C., & Wang, H. (2007). High-resolution proxy record of Holocene climate  
 430 from a loess section in Southwestern Nebraska, USA. *Palaeogeography, Palaeoclimatology,*  
 431 *Palaeoecology*, *245*(3–4), 368–381. <https://doi.org/10.1016/j.palaeo.2006.09.004>
- 432 Morrill, C., Lowry, D. P., & Hoell, A. (2018). Thermodynamic and Dynamic Causes of Pluvial Conditions During  
 433 the Last Glacial Maximum in Western North America. *Geophysical Research Letters*, *45*(1), 335–345.  
 434 <https://doi.org/10.1002/2017GL075807>
- 435 O’Brien, S. R., Mayewski, P., Meeker, L. D., Twickler, M. S., & Whitlow, S. I. (1995). Complexity of Holocene  
 436 climate as reconstructed from a Greenland ice core. *Science*, *270*, 1962.
- 437 Olsen, J., Anderson, N. J., & Knudsen, M. F. (2012). Variability of the North Atlantic Oscillation over the past  
 438 5,200 years. *Nature Geoscience*, *5*(11), 808–812. <https://doi.org/10.1038/ngeo1589>
- 439 Orme, L. C., Miettinen, A., Seidenkrantz, M.-S., Tuominen, K., Pearce, C., Divine, D. V., et al. (2021). Mid to late-  
 440 Holocene sea-surface temperature variability off north-eastern Newfoundland and its linkage to the North  
 441 Atlantic Oscillation. *The Holocene*, *31*(1), 3–15. <https://doi.org/10.1177/0959683620961488>
- 442 Oswald, W. W., Faison, E. K., Foster, D. R., Doughty, E. D., Hall, B. R., & Hansen, B. C. S. (2007). Post-glacial  
 443 changes in spatial patterns of vegetation across southern New England. *Journal of Biogeography*, *34*(5),  
 444 900–913. <https://doi.org/10.1111/j.1365-2699.2006.01650.x>

- 445 Oswald, W. W., Foster, D. R., Shuman, B. N., Doughty, E. D., Faison, E. K., Hall, B. R., et al. (2018). Subregional  
446 variability in the response of New England vegetation to postglacial climate change. *Journal of*  
447 *Biogeography*, 45(10), 2375–2388. <https://doi.org/10.1111/jbi.13407>
- 448 Overpeck, J. T., Webb III, T., & Prentice, I. C. (1985). Quantitative interpretation of fossil pollen spectra:  
449 dissimilarity coefficients and the method of modern analogs. *Quaternary Research*, 23, 87–108.
- 450 Paciorek, C. J., Goring, S. J., Thurman, A. L., Cogbill, C. V., Williams, J. W., Mladenoff, D. J., et al. (2016).  
451 Statistically-estimated tree composition for the northeastern United States at Euro-American settlement.  
452 *PloS One*, 11(2), e0150087.
- 453 Paciorek, C. J., Cogbill, C. V., Peters, J. A., Williams, J. W., Mladenoff, D. J., Dawson, A., & McLachlan, J. S.  
454 (2021). The forests of the midwestern United States at Euro-American settlement: Spatial and physical  
455 structure based on contemporaneous survey data. *PLOS ONE*, 16(2), e0246473.  
456 <https://doi.org/10.1371/journal.pone.0246473>
- 457 Parnell, A. C., Haslett, J., Allen, J. R. M., Buck, C. E., & Huntley, B. (2008). A flexible approach to assessing  
458 synchronicity of past events using Bayesian reconstructions of sedimentation history. *Quaternary Science*  
459 *Reviews*, 27(19), 1872–1885. <https://doi.org/10.1016/j.quascirev.2008.07.009>
- 460 Pielke, R. A., & Vidale, P. L. (1995). The boreal forest and the polar front. *Journal of Geophysical Research:*  
461 *Atmospheres*, 100(D12), 25755–25758. <https://doi.org/10.1029/95JD02418>
- 462 Portis, D. H., Walsh, J. E., El Hamly, M., & Lamb, P. J. (2001). Seasonality of the North Atlantic Oscillation.  
463 *Journal of Climate*, 14(9), 2069–2078.
- 464 Prentice, I. C., Bartlein, P. J., & Webb III, T. (1991). Vegetation and climate changes in eastern North America  
465 since the last glacial maximum: A response to continuous climatic forcing. *Ecology*, 72, 2038–2056.
- 466 R Core Development Team. (2022). *R: A language and environment for statistical computing*. R Foundation for  
467 Statistical Computing, Vienna, Austria. Retrieved from <http://www.R-project.org>
- 468 Reimer, P. J., Austin, W. E. N., Bard, E., Bayliss, A., Blackwell, P. G., Ramsey, C. B., et al. (2020). The IntCal20  
469 Northern Hemisphere Radiocarbon Age Calibration Curve (0–55 cal kBP). *Radiocarbon*, 62(4), 725–757.  
470 <https://doi.org/10.1017/RDC.2020.41>
- 471 Renssen, H., Goosse, H., & Muscheler, R. (2006). Coupled climate model simulation of Holocene cooling events:  
472 oceanic feedback amplifies solar forcing. *Climate of the Past*, 2, 79–90.

- 473 Rigor, I. G., Wallace, J. M., & Colony, R. L. (2002). Response of Sea Ice to the Arctic Oscillation. *Journal of*  
474 *Climate*, 15(18), 2648–2663. [https://doi.org/10.1175/1520-0442\(2002\)015<2648:ROSITT>2.0.CO;2](https://doi.org/10.1175/1520-0442(2002)015<2648:ROSITT>2.0.CO;2)
- 475 Routson, C. C., McKay, N. P., Kaufman, D. S., Erb, M. P., Goosse, H., Shuman, B. N., et al. (2019). Mid-latitude  
476 net precipitation decreased with Arctic warming during the Holocene. *Nature*, 568(7750), 83–87.  
477 <https://doi.org/10.1038/s41586-019-1060-3>
- 478 Ruddiman, W. F., & McIntyre, A. (1981). The North Atlantic Ocean during the last deglaciation. *Palaeogeography,*  
479 *Palaeoclimatology, Palaeoecology*, 35, 145–214.
- 480 Schmidt, M. W., Weinlein, W. A., Marcantonio, F., & Lynch-Stieglitz, J. (2012). Solar forcing of Florida Straits  
481 surface salinity during the early Holocene. *Paleoceanography*, 27(3).  
482 <https://doi.org/10.1029/2012PA002284>
- 483 Seager, R., Battisti, D. S., Yin, J., Gordon, N., Naik, N., Clement, A. C., & Cane, M. A. (2002). Is the Gulf Stream  
484 responsible for Europe’s mild winters? *Quarterly Journal of the Royal Meteorological Society*, 128(586),  
485 2563–2586. <https://doi.org/10.1256/qj.01.128>
- 486 Shuman, B. N. (2022). Centennial-to-Millennial Holocene Temperature and Hydroclimate Variation in the Northern  
487 Mid-Latitudes. *Climates of the Past Discussion*. <https://doi.org/10.5194/cp-2022-89>
- 488 Shuman, B. N., & Marsicek, J. P. (2016). The Structure of Holocene Climate Change in Mid-Latitude North  
489 America. *Quaternary Science Reviews*, 141, 38–51.
- 490 Shuman, B. N., Bartlein, P., Logar, N., Newby, P., & Webb, T. (2002). Parallel climate and vegetation responses to  
491 the early-Holocene collapse of the Laurentide Ice Sheet. *Quaternary Science Reviews*, 21, 1793–1805.
- 492 Shuman, B. N., Marsicek, J., Oswald, W. W., & Foster, D. R. (2019). Predictable hydrological and ecological  
493 responses to Holocene North Atlantic variability. *Proceedings of the National Academy of Sciences*,  
494 116(13), 5985–5990. <https://doi.org/10.1073/pnas.1814307116>
- 495 Thompson, J. R., Carpenter, D. N., Cogbill, C. V., & Foster, D. R. (2013). Four Centuries of Change in Northeastern  
496 United States Forests. *PLOS ONE*, 8(9), e72540. <https://doi.org/10.1371/journal.pone.0072540>
- 497 Thompson, L. G., Mosley-Thompson, E., Davis, M. E., Henderson, K. A., Brecher, H. H., Zagorodnov, V. S., et al.  
498 (2002). Kilimanjaro Ice Core Records: Evidence of Holocene Climate Change in Tropical Africa. *Science*,  
499 298(5593), 589–593. <https://doi.org/10.1126/science.1073198>

- 500 Thornalley, D. J. R., Elderfield, H., & McCave, I. N. (2009). Holocene oscillations in temperature and salinity of the  
501 surface subpolar North Atlantic. *Nature*, *457*(7230), 711–714.
- 502 Vanni re, B., Power, M. J., Roberts, N., Tinner, W., Carri n, J., Magny, M., et al. (2011). Circum-Mediterranean  
503 fire activity and climate changes during the mid-Holocene environmental transition (8500-2500 cal. BP).  
504 *The Holocene*, *21*(1), 53–73. <http://dx.doi.org.libproxy.uwyo.edu/10.1177/0959683610384164>
- 505 Whitehead, D. R., & Crisman, T. (1978). Paleolimnological studies of small New England (U.S.A.) ponds. I: Late  
506 glacial and postglacial trophic oscillations. *Polskie Archiwum Hydrobiologii*, *25*, 471–481.
- 507 Whitmore, J., Gajewski, K., Sawada, M., Williams, J., Shuman, B., Bartlein, P. J., et al. (2005). An updated modern  
508 pollen-climate-vegetation dataset for North America. *Quaternary Science Reviews*, *24*, 1828–1848.
- 509 Willard, D. A., Bernhardt, C. E., Korejwo, D. A., & Meyers, S. R. (2005). Impact of millennial-scale Holocene  
510 climate variability on eastern North American terrestrial ecosystems: pollen-based climatic reconstruction.  
511 *Global and Planetary Change*, *47*(1), 17–35. <https://doi.org/10.1016/j.gloplacha.2004.11.017>
- 512 Williams, J. W., Shuman, B. N., Bartlein, P. J., Whitmore, J., Gajewski, K., Sawada, M., et al. (2006). An Atlas of  
513 Pollen-Vegetation-Climate Relationships for the United States and Canada. *American Association of*  
514 *Stratigraphic Palynologists Foundation, Dallas, TX*.
- 515 Williams, J. W., Grimm, E. C., Blois, J. L., Charles, D. F., Davis, E. B., Goring, S. J., et al. (2018). The Neotoma  
516 Paleocology Database, a multiproxy, international, community-curated data resource. *Quaternary*  
517 *Research*, *89*(1), 156–177. <https://doi.org/10.1017/qua.2017.105>
- 518 Woodward, F. I. (1987). *Climate and Plant Distribution*. (R. S. K. Barnes, H. J. B. Birks, E. F. Connor, J. L. Harper,  
519 & R. T. Paine, Eds.). Cambridge: Cambridge University Press.
- 520 Vose, R.S., Applequist, S., Durre, I., Menne, M.J., Williams, C.N., Fenimore, C., et al. (2014). Improved Historical  
521 Temperature and Precipitation Time Series For U.S. Climate Divisions. *Journal of Applied Meteorology*  
522 *and Climatology*. <http://dx.doi.org/10.1175/JAMC-D-13-0248.1>

523

524